Journal of Hazardous Materials 211–212 (2012) 373–380

Contents lists available at SciVerse ScienceDirect

Journal of Hazardous Materials

journal homepage: www.elsevier.com/locate/jhazmat

Biodegradable surfactant stabilized nanoscale zero-valent iron for in situ treatment of vinyl chloride and 1,2-dichloroethane

Yu-Ting Wei [a], Shian-chee Wu [a], Shi-Wei Yang [a], Choi-Hong Che [a], Hsing-Lung Lien [b,*], De-Huang Huang [c]

[a] Graduate Institute of Environmental Engineering, National Taiwan University, Taipei, Taiwan, ROC
[b] Department of Civil and Environmental Engineering, National University of Kaohsiung, Kaohsiung, Taiwan, ROC
[c] Chinese Petroleum Corporation, Kaohsiung, Taiwan, ROC

ARTICLE INFO

Article history:
Received 15 June 2011
Received in revised form 2 November 2011
Accepted 3 November 2011
Available online 10 November 2011

Keywords:
Nanoscale zero-valent iron
Biodegradable dispersant
Nonionic surfactant
Vinyl chloride monomer manufacturing
Dichloroethane
Groundwater pollution

ABSTRACT

Nanoscale zero-valent iron (NZVI) stabilized with dispersants is a promising technology for the remediation of contaminated groundwater. In this study, we demonstrated the use of biodegradable surfactant stabilized NZVI slurry for successful treatment of vinyl chloride (VC) and 1,2-dichloroethane (1,2-DCA) in a contaminated site in Taiwan. The biodegradable surfactant stabilized NZVI was coated with palladium and synthesized on-site. From monitoring the iron concentration breakthrough and distribution, it was found that the stabilized NZVI is capable of transporting in the aquifer at the test plot (200 m^2). VC was effectively degraded by NZVI while the 1,2-DCA degradation was relatively sluggish during the 3-month field test. Nevertheless, as 1,2-DCA is known to resist abiotic reduction by NZVI, the observation of 1,2-DCA degradation and hydrocarbon production suggested a bioremediation took place. ORP and pH results revealed that a reducing condition was achieved at the testing area facilitating the biodegradation of chlorinated organic hydrocarbons. The bioremediation may be attributed to the production of hydrogen gas as electron donor from the corrosion of NZVI in the presence of water or the added biodegradable surfactant serving as the carbon source as well as electron donor to stimulate microbial growth.

1. Introduction

Using metallic or bimetallic nanoparticles for the remediation of chlorinated aliphatic hydrocarbons (CAHs) contaminated groundwater is one of the most significant applications in the environmental nanotechnology. Among many metallic nanoparticles, nanoscale zero-valent iron (NZVI) can be readily produced by the reduction of dissolved iron using sodium borohydride solutions or by milling or grinding process [1,2]. Field and laboratory experiments have demonstrated that NZVI with its high specific surface areas is an effective reducing reagent for the dechlorination of CAHs in aqueous systems such as tetrachloroethylene, trichloroethylene (TCE), 1,1,1-trichloroethane, carbon tetrachloride, and chloroform [3–7]. Additionally, NZVI coated with second catalytic metals such as palladium (Pd) or nickel (Ni) has shown the ability to facilitate the efficiency of dechlorination and to prevent the formation of toxic byproducts (e.g. vinyl chloride (VC)) [6,7].

In the absence of dispersants, NZVI tends to aggregate, which poses a challenge to deliver NZVI into the subsurface for the remediation of groundwater contaminated with CAHs. To overcome this limitation, a wide array of dispersants has been tested to disperse NZVI including cationic, anionic and nonionic surfactants [8–11]. The stabilization of the surfactants has been attributed to their surface-active properties, which can alter the electrostatic charges to increase the repulsion between two adjacent particles. In addition, particles covered with polymers [12,13] could also stay stably in aqueous phase due to steric hindrance, which reduces the probability of successful collision and subsequent coagulation. Among them, poly acrylic acid (PAA) is one of the most effective dispersants widely used. Besides dispersibility, the affinity for the oil/water interface is another significant factor influencing the remediation of dense non-aqueous phase liquids (DNAPLs) source. Saleh et al. has reported that triblock copolymers cannot only promote NZVI stability but also drive NZVI to the DNAPLs/water interface for directly attacking and removing the source zone [14].

The concentrations of dispersants applied in the above studies varied in a wide range from mg/L to percentage. When the NZVI slurry is injected in situ, a comparable amount of dispersants is also added into the subsurface. Thus, the impacts on the environment caused by the dispersants should be taken into account. Extensive studies have applied biodegradable surfactant and polymer for the stabilization of NZVI [13,15]. Natural materials such as starch and soy protein have also been reported capable of stabilizing NZVI [16,17]. Besides the environment friendly characteristic, biodegradable surfactants may offer a synergistic effect in NZVI treatment due to the enhanced bioactivity. It has been

* Corresponding author. Tel.: +886 7591 9221; fax: +886 7591 9376.
E-mail address: lien.sam@nuk.edu.tw (H.-L. Lien).

0304-3894/$ – see front matter © 2011 Elsevier B.V. All rights reserved.
doi:10.1016/j.jhazmat.2011.11.018

reported that the injection of NZVI into saturated porous media creates a reducing condition, with an oxidation–reduction potential (ORP) at a low level (−300 to −500 mV) [18,19]. While the reducing conditions are likely beneficial to an anaerobic bioremediation, the additional biodegradable surfactants would provide sufficient carbon sources to sustain bacteria growth. Several types of surfactants have been found with high anaerobic biodegradability, such as sulphated anionic surfactants, alcohol ethoxylates, alkylethanolamides, alkyldimethyl amine oxides, and amphoteric surfactants [20]. Of which, alkylethanolamides were considered adoptable to use as the dispersant and biostimulation reagent for the present study.

While the well-controlled laboratory studies have already provided many insights into the understanding of fundamental chemistry and mechanisms of NZVI, the knowledge gained from the field studies is valuable and of at least equal, if not greater importance, with regard to the application of NZVI. In our previous report, we have shown the influence of NVZI on geochemical properties of groundwater and VC degradation in the testing site [19]; nevertheless, the influence of biodegradable surfactant on the CAHs degradation by NZVI has not yet been discussed. In this study, an in situ treatment experiment using on-site synthesized NZVI stabilized with the biodegrable surfactant was implemented at a 200 m^2 pilot site. Palladized commercial NZVI dispersed by PAA was also conducted to perform the comparison of reactivity. In order to compare the reactivity of abiotic and biotic degradation, a test site contaminated primarily with VC and 1,2-dichloroethane (1,2-DCA) was selected. While extensive studies have indicated that VC is readily dechlorinated to ethylene using palladized NZVI [21–23], 1,2-DCA with low reaction rates ($\sim 5.0 \times 10^{-5}$ 1/h) resisted to be reduced under the same abiotic way [24]. Thus, the observation of 1,2-DCA dechlorination at this site could serve as a supporting evidence of enhanced biodegradation by surfactant stabilized NZVI. To conduct a systematic study, thirteen nested multi-level monitoring wells were installed to analyze geochemical parameters and contaminant concentrations in groundwater. A breakthrough test and monitoring transport of NZVI were also conducted to evaluate the mobility and distribution of modified NZVI.

2. Experimental

2.1. Site description

The potential pollution source in the pilot test site came from a vinyl chloride monomer (VCM) manufacturing plant located in southern Taiwan. The NZVI pilot test was conducted in a small plot (10 m × 20 m) south of the VCM plant in the groundwater downstream direction. The primary contaminant inside the plant is 1,2-DCA. However, high concentrations of VC (46.7 ± 4.16 μM), 1,2-DCA (2.0 ± 0.51 μM), 1,1-dichloroethane (4.4 ± 0.41 μM), 1,1-dichloroethylene (3.8 ± 1.1 μM), *cis*-1,2-dichloroethylene (9.8 ± 3.5 μM) and TCE (4.3 ± 1.5 μM) in groundwater were detected from the monitoring well nearby the plant and in groundwater downstream direction. At the test plot, the unconfined aquifer, composed of medium to coarse sand and few silt, lies approximately 4–18 m below ground surface (m bgs). The detailed geohydraulic parameters can be found in our previous publication [19].

2.2. NZVI test plot design

Three injection wells and thirteen nested multi-level monitoring wells were installed within the 200 m^2 plot. There was one nested monitoring well located upstream for the purpose of background monitoring. In the downstream direction of each injection well, four multi-level monitoring wells were installed. The positions of the four nested monitoring wells were approximately 1, 2, 3, and 5 m from the injection well. The injection wells were 18 m deep with 15 m screens. Every nested monitoring well was embedded with three separate wells, at approximately 6, 12 and 18 m deep with 3 m screens (Fig. 1). The three separate wells at different descending levels are referred to as upper, middle, and bottom layers in this paper to indicate the position of each sample.

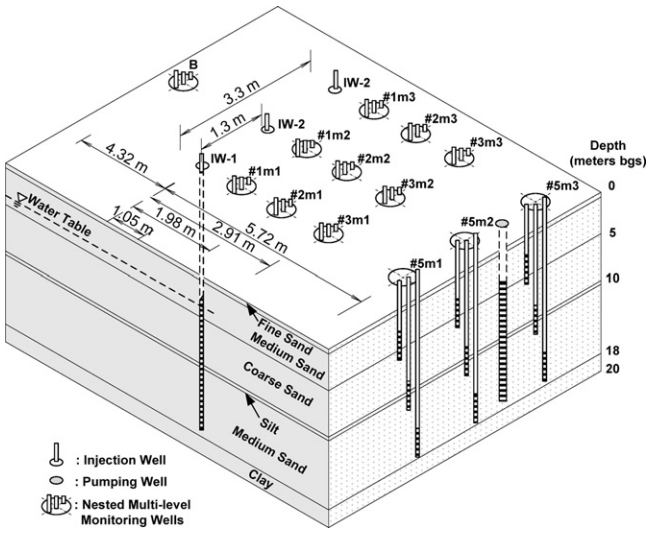

Fig. 1. Injection and monitoring locations within NZVI test plot.

2.3. Field experiment setup

Two types of NZVI were applied in two separate rounds (Fig. 2). The field chronology is listed in Table 1. There was a five-month interval between two rounds to minimize cross interference. In Round 1, commercial NZVI slurry purchased from Lehigh Nanotech LLC was diluted to 2250 L at the NZVI concentration of 17.8 g iron/L and injected into Well IW-2 via gravity. The commercial NZVI was dispersed by PAA and the total iron mass was 40 kg with an additional 400 g of palladium catalyst (1% of total iron mass). Prior to the start of Round 2, 1000 L of 5000 mg/L nonionic surfactant solution was injected to condition the aquifer. In Round 2, 1000 L of the on-site synthesized NZVI stabilized with a nonionic surfactant, industrial-grade coconut fatty acid diethanolamide ($C_{11}H_{23}CO–N(CH_2CH_2OH)_2$) were first injected into Well IW-3 by

Table 1
Summary of field chronology.

Round	Days after injection	Event
1	0	Commercial NZVI injection into IW-2
	6	Performance monitoring
	14	Performance monitoring
	34	Performance monitoring
	47	Performance monitoring
	68	Performance monitoring
	103	Performance monitoring
2	0	On-site synthesized NZVI injection into IW-3
	4	Performance monitoring
	10	On-site synthesized NZVI injection into IW-1, Breakthrough monitoring
	11	Performance monitoring
	25	Performance monitoring
	36	Performance monitoring
	63	Performance monitoring
	97	Performance monitoring

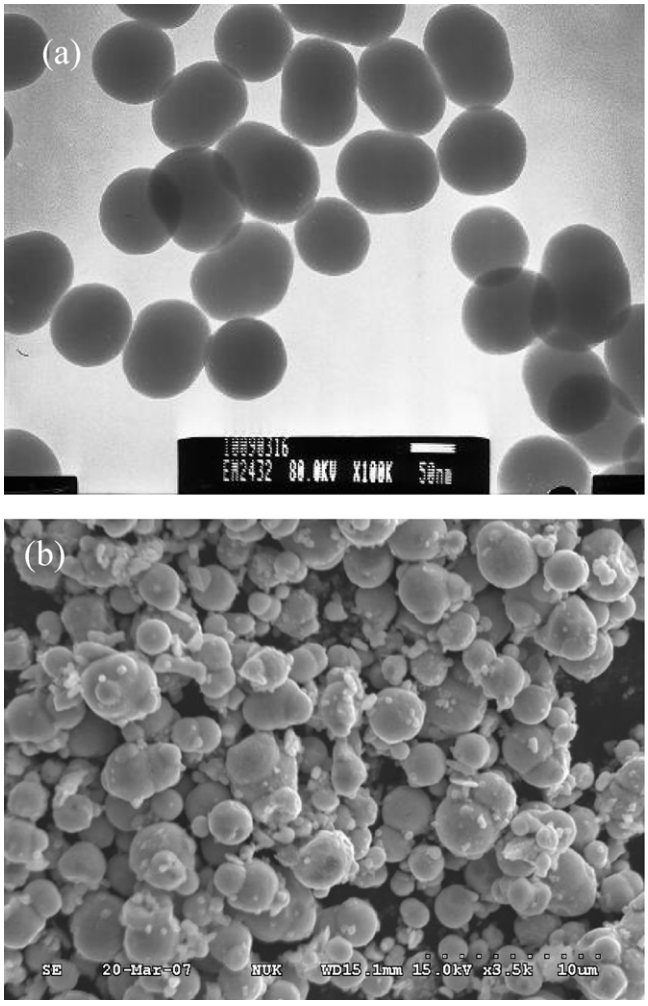

Fig. 2. (a) The TEM picture of on-site synthesized NZVI and (b) the SEM picture of commercial NZVI.

gravity. The detailed process of preparation of on-site synthesized NZVI can be referred to our previous publication [19]. Due to a rapid breakthrough to ground occurred around IW-3, another 7500 L of NZVI suspension was injected into IW-1 via gravity after 10 days to investigate the breakthrough of NZVI. The concentration of on-site synthesized NZVI was about 2.5 g iron/L, corresponding to 20 kg of iron mass companioned with 100 g of palladium catalyst (0.5% of total iron mass) injected in Round 2. Groundwater (16,500 L) withdrawn from the pumping well close to the nested well #5 m^2 was injected into IW-1 to circulate the injected NZVI for 29 h.

2.4. Sample analytic methods

The groundwater samples were collected at various time intervals to monitor the performance of the field tests. ORP and pH were measured by a portable YSI 650 MDS-6600 V2-4 Sonde equipment (YSI Inc.). A TOC analyzer (TOC 101, OI Corporation) was used to measure TOC. Total dissolved iron was detected by UV detector at 562 nm by adding ascorbic acid (1% w/v) and ferrozine (3-(2-pyridyl)-5,6-bis (4-phenylsulfonic acid)-1,2,4-triazine) to a 0.45 μm-membrane-filtered sample. Total iron was measured by atomic absorption spectrophotometer (PerkinElmer Analyst 800) after acid digestion. TOC was measured to represent the concentration of the surfactant. Volatile organic compounds were measured by GC/MS (Angilent 6890/5973 with a 60 m DB-624 capillary column) using a purge and trap sampling equipment (OI Analytical. Model 4560). Methane, ethane and ethylene were first equilibrated at 25 °C in the headspace of 20 mL serum vial containing 10 mL of the water sample, and were then analyzed by GC/FID (HP 5890 with a 60 m GS-GASPRO column). The concentrations of these target gases were calculated following the guidelines of US EPA report [25].

2.5. Solid-phase characterization

Morphological and elemental analyses of NZVI were performed by scanning and transmission electron microscope (SEM and TEM). A Hitachi S-4300 SEM (Hitachi Science Systems, Ltd.) equipped with energy-dispersive X-ray (EDX) analysis (at 10 kV) and a TEM (JEOL JSM-1200EX II) were applied. Beckman Coulter SA3100 surface area analyzer was used to measure surface areas with the N_2-adsorption-BET method. Fourier transform infrared spectrometer (FTIR) (Nexus 470, Thermo Nicolet, USA) equipped with a DTGS detector (wave number range 400–4000 cm^{-1}) was used to investigate the interaction between surfactant and reductive reagent. Sixteen scans per samples were recorded, averaged and corrected against the spectrum of pure KBr as the background. The hydrodynamic diameter of synthesized NZVI was measured by ZetaSizer instrument (3000HS, Malvern).

3. Results and discussion

3.1. Characterization of synthesized and commercial available NZVI

Fig. 2 shows the TEM and SEM images of synthesized NZVI and commercial NZVI, respectively. The on-site synthesized NZVI has particle sizes in the range of 80–120 nm whereas the commercial NZVI has particle sizes between 450 and 550 nm. The elemental analysis conducted by SEM-EDX revealed that the iron content accounted for nearly 100 wt% of commercial NZVI. The average hydrodynamic diameter of synthesized NZVI measured by ZetaSizer was 400 nm that reflected the size of the surfactant forming aggregation of micelles [26]. The specific surface area of on-site synthesized NZVI stabilized with the surfactant was measured to be about 29.3 m^2/g, close to that dispersed by PAA at 20–30 m^2/g [12], but significantly lower than that dispersed by starch at 55 m^2/g [16]. However, the specific surface area of commercial NZVI was considerably low (~4.61 m^2/g).

Fig. 3 illustrates the FTIR spectra of the surfactant with $NaBH_4$ and the surfactant with stabilized NZVI. The peaks of the surfactant with $NaBH_4$ appeared at approximately 3404, 2936, and 1650 cm^{-1}, corresponding to OH, CH_2 (long chain fatty acids), and amide C=O stretching vibration, respectively. This is consistent with the chemical structure of coconut fatty acid diethanolamide. A small shift in peaks such as amide C=O stretching vibration from 1650 cm^{-1} to 1632 cm^{-1} observed in the surfactant stabilized NZVI indicating the interaction between the surfactant and NZVI occurred.

Laboratory batch tests showed that the surfactant stabilized NZVI with palladium had a rapid and complete dechlorination of VC (40 μM) within one hour. The addition of the surfactant did not decrease the degradation rates of contaminants. Furthermore, the surfactant applied in this study is biodegradable under aerobic conditions as Madsen et al. reported that it is fully degradable in a 28-day standard test of biodegradability [27]. Previous studies had also depicted that the biodegradation of the surfactant exhibits a lag phase under anaerobic conditions, which is dependent on the concentration of surfactants [28]. The effect may be attributed to a selective inhibition in the methanogenic activity. Long-chain fatty acids such as the hydrophobic group of surfactants

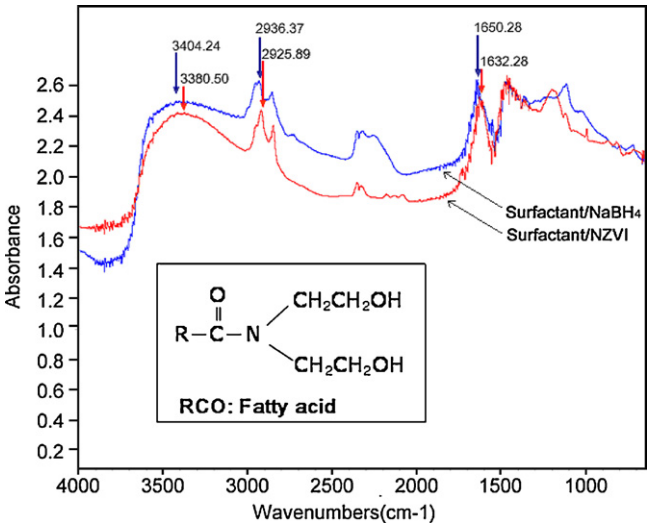

Fig. 3. The FTIR spectra of surfactants interacted with $NaBH_4$ and NZVI. Inset shows the molecular structure of the surfactant.

metabolized from the alkylethanolamide might be recognized as being inhibitory to methanogenic bacteria [29,30].

3.2. Breakthrough of NZVI in the field

To evaluate the mobility of the surfactant stabilized NZVI, a breakthrough test of NZVI was performed by monitoring the iron and TOC concentrations in the vicinity of the injection well. The injection well IW-1 and the monitoring well #1 m^2 were selected, with a distance of 1.67 m in-between. As shown in Fig. 4, it was found that the concentrations of TOC and iron in the middle and bottom layers reached their peaks when the total volume of the injection was at 19,000 L. However, the breakthrough of TOC or iron

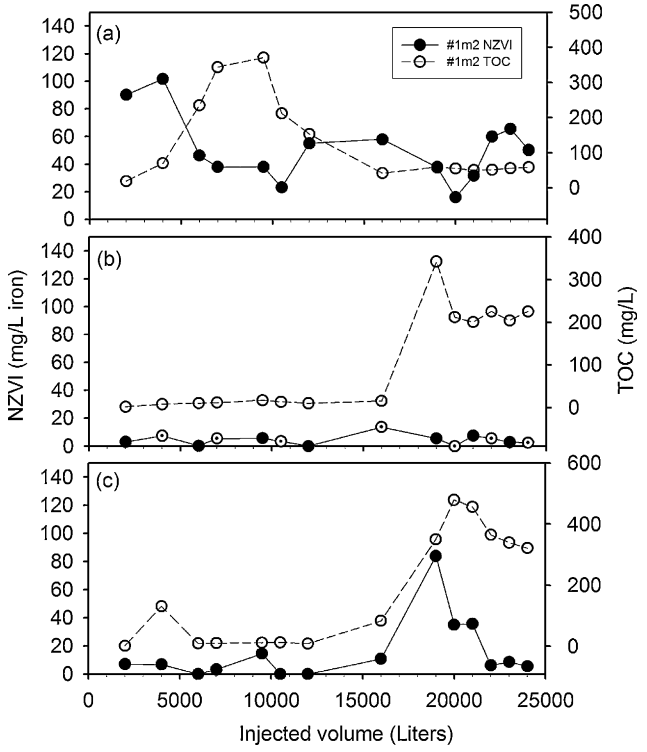

Fig. 4. Breakthrough concentrations of NZVI and TOC in accumulative Run in (a) upper, (b) middle, and (c) bottom layers.

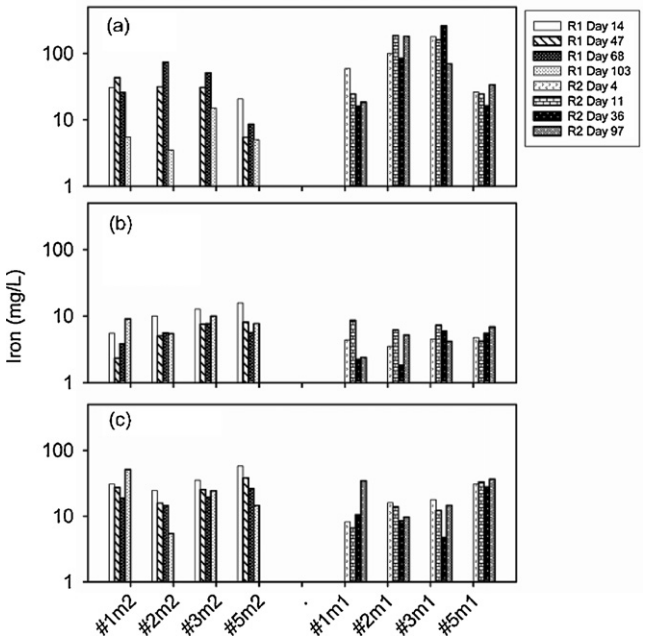

Fig. 5. Total iron concentrations in Round 1 (R1) and Round (R2) in (a) upper, (b) middle, and (c) bottom layers.

was found in the upper layer at an earlier stage of the injection. The early accumulation of NZVI may be resulted from a large portion of NZVI seeping through channels in the unsaturated zone [19]. Hence the initial NZVI concentration declined in the middle and bottom layers. Considering the initial TOC concentration of the surfactant stabilized NZVI and measured concentration in the bottom layer were at about 4000 and 456 mg/L, respectively, a dilution rate of 1:9 can be estimated. Therefore, it is reasonable to assume that the initial NZVI concentration at the injection well was diluted at the same rate of 1:9, from 2500 to 278 mg/L in the bottom layer. By applying the classical colloid filtration theory [31], the NZVI concentration at the monitoring well #1 m^2 can be predicted by applying:

$$C = C_0 \times e^{-\lambda L} \quad (1)$$

where C is the NZVI concentration, C_0 is the initial concentration of NZVI, L is the transport length of soil and λ is the filter coefficient. Our previous study with similar NZVI suspension for a breakthrough test suggested λ is 0.828 m^{-1} using a 0.3 m soil column [26]. Thus, the estimated NZVI concentration in the bottom layer was calculated to be about 69.7 mg/L, which is close to measured concentration of 83.9 mg/L.

3.3. Spatial distribution of iron

Fig. 5 shows the spatial distribution of total iron concentration measured by sampling from monitored wells located down-gradient from the injection well during Round 1 and Round 2. As shown in Fig. 5, it is clear that the iron concentration found in the upper layer was significantly higher than that found in the middle and bottom layers. This suggested that NZVIs were largely trapped in the upper layer and did not penetrate to the lower layers. In comparing the upper layers between Round 1 and Round 2, a higher iron concentration was found in Round 2. This may be attributed to the low-volume injection method that could cause a decrease in the mobility of the commercial NZVI. As illustrated in Fig. 5(a), the iron concentration showed a tendency of decrease towards downstream. At the farthest down-gradient well (5 m apart from the injection well), it was found that the iron concentration was essentially no different from the background iron

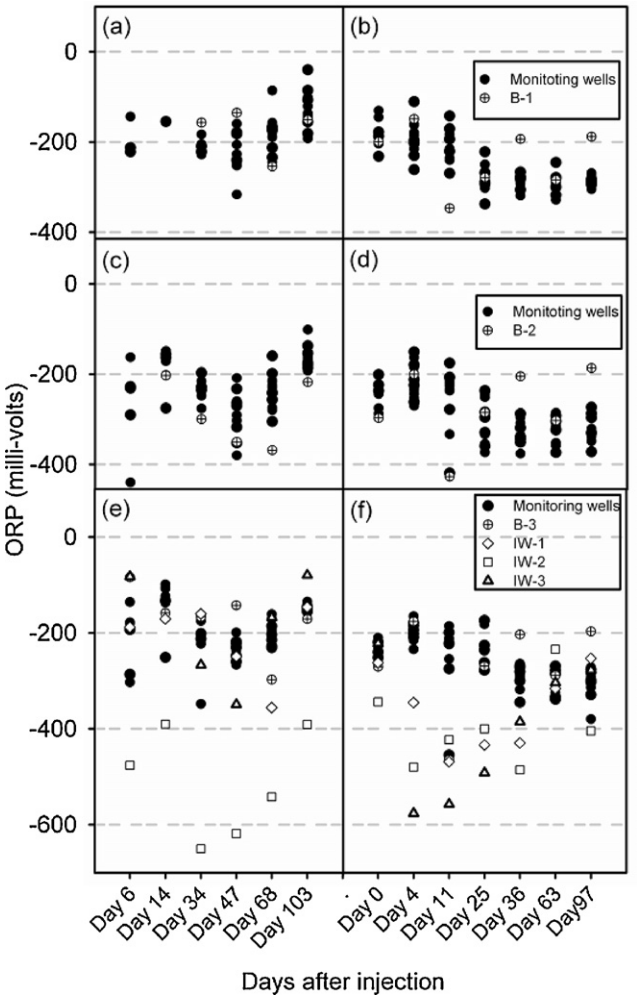

Fig. 6. ORP in Round 1 (left column) and Round 2 (right column) in (a) (b) upper, (c) (d) middle, and (e) (f) bottom layers.

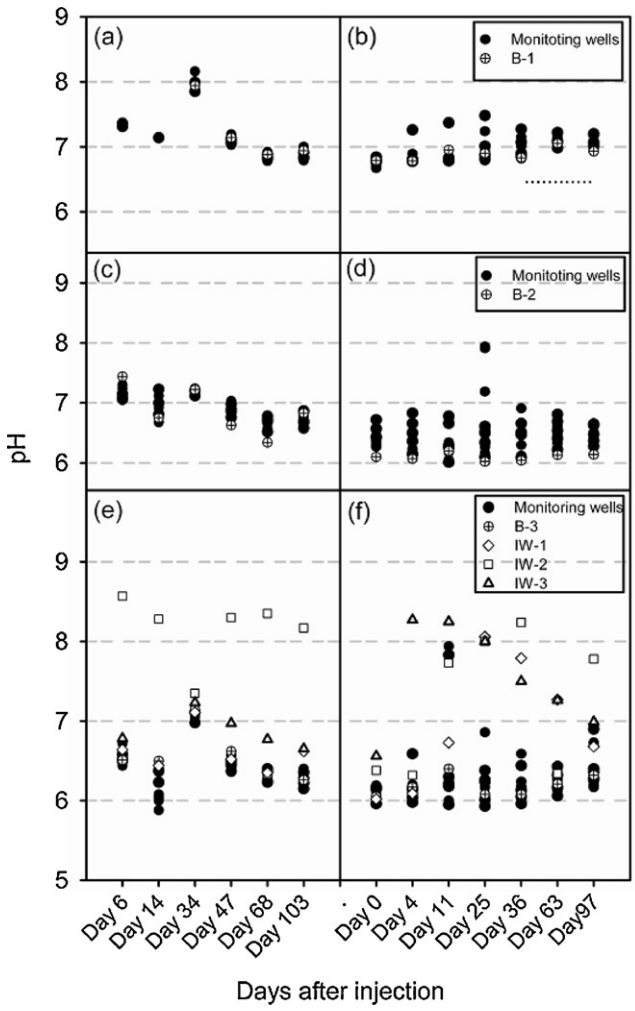

Fig. 7. pH in Round 1 (left column) and Round 2 (right column) in (a) (b) upper, (c) (d) middle, and (e) (f) bottom layers.

concentration suggesting the travel distance of NZVI is no further than 5 m. Though this study is not aimed at exploring the change of the morphology or composition of NZVI, the agglomeration of NZVI observed in the SEM image of soil samples may account for the limitation of NZVI transport [19].

3.4. Changes in ORP and pH

The E_h and pH profiles at given locations over time can be used as convenient indicators for NZVI reactivity [18,19,32]. As illustrated in Fig. 6, ORP detected during Round 2 after injection was significantly lower than that during Round 1. The injection wells in both rounds maintained at a lower level of ORP (<−400 mV) indicating that strong-reducing conditions suitable for the reductive dehalogenation was established. The initial background ORP was found at between −100 and −300 mV, which indicated reducing conditions in groundwater aquifer at this site prior to the field study.

During Round 1, ORP in the middle layer was found to be consistently below −200 mV, while those in the upper and bottom layers fell somewhere above −200 mV. Many factors may have contributed to these differences in ORP. Silt found in the middle layer may have made it more vulnerable in accumulating plant debris and organic contents such as humic acids for biotic reactions [33] or iron pyrite precipitates for abiotic reactions [34], which all may encourage an anaerobic condition.

The pH value was expected to increase when the oxidation of zero-valent iron took place and hydroxyl ions were produced [35]. As shown in Fig. 7, there was a slight increase in the pH value in the upper layer as opposed to an unnoticeable increase in the pH value in either the middle or bottom layer. In general, the pH value was maintained in the range of 6–8 during the testing period, suggesting that NZVI remained reactive in the testing site. The relatively low pH condition is in agreement with the observation of a 1,2-DCA contaminated site in natural attenuation conditions reported by Nobre and Nobre [36]. Furthermore, the pH measured in this field study is within the optimum range for the biodegradation of chlorinated solvents [37].

3.5. Reduction of VC and 1,2-DCA

The concentrations of VC monitored at different time periods for the three layers at selected wells are summarized in Fig. 8. The concentration distribution of VC at the testing site was depth-dependent, where contaminant concentrations increased with depth. For example, VC concentration at the upper layer was in the range of 0.5–10 μM while VC at the bottom layer can reach a concentration greater than 100 μM. It should be pointed out that a pumping test was conducted to determine the geohydraulic parameters during the break between Round 1 and Round 2. This may change the flow conditions of the aquifer, which may further explain the substantial difference between initial VC

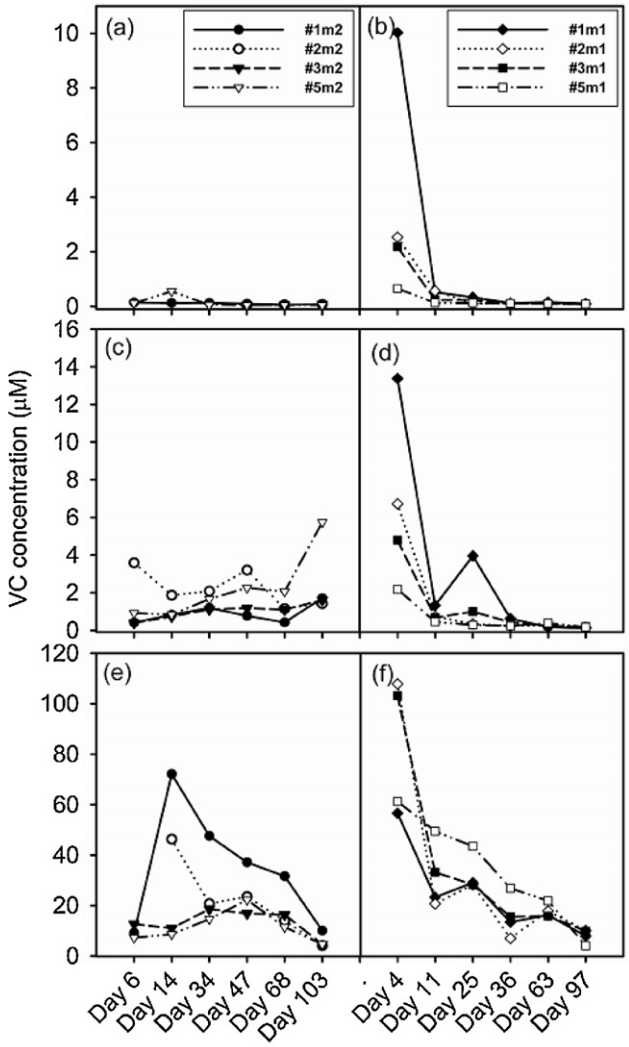

Fig. 8. VC concentrations in Round 1 (left column) and Round 2 (right column) in (a) (b) upper, (c) (d) middle, and (e) (f) bottom layers.

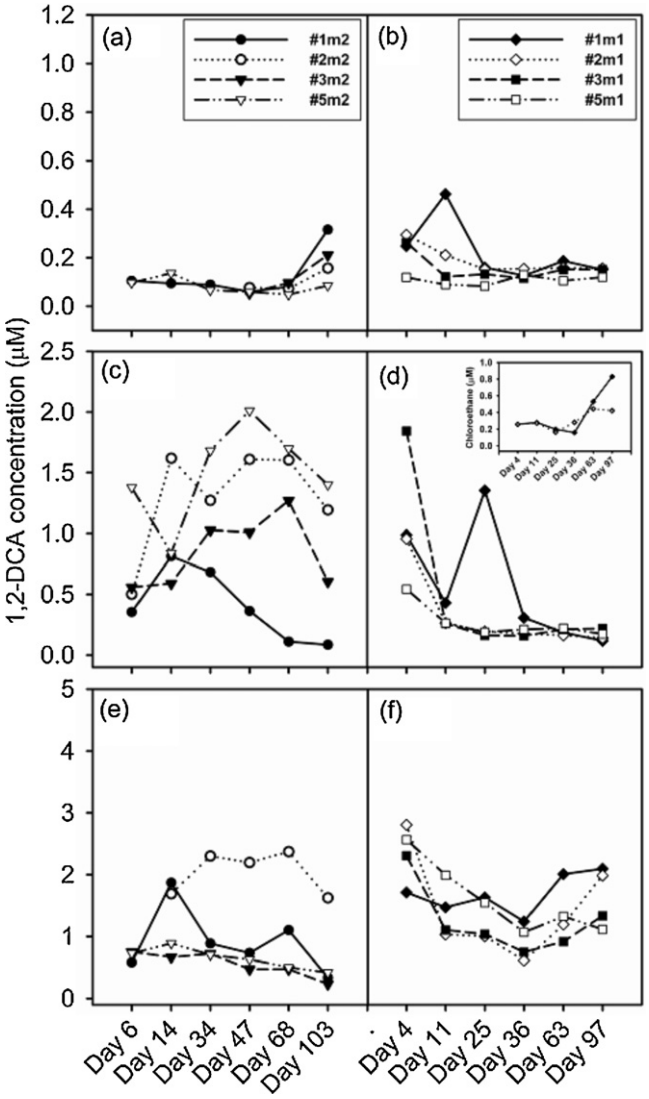

Fig. 9. 1,2-DCA concentrations in Round 1 (left column) and Round 2 (right column) in (a) (b) upper, (c) (d) middle, and (e) (f) bottom layers. Inset (d) shows chloroethane concentration.

concentrations found in the two rounds. Nevertheless, VC concentrations showed a gradual decline in both rounds. Fig. 8 also reveals that the on-site synthesized NZVI (Round 2) performed better than the commercially available NZVI (Round 1). This may be attributed to the higher surface areas and relatively fresh surface for the on-site synthesized NZVI. According to the study conducted by Maymo-Gatell et al. [38], anaerobic dihaloelimination of 1,2-DCA is able to produce up to 1% of VC as an intermediate but mostly as ethylene. The higher concentration of VC accumulated at the down-gradient source of 1,2-DCA implied that the biodegradation has already existed prior to the injection of NZVI.

Compared to VC, 1,2-DCA showed a relatively lower concentration at the testing site, as shown in Fig. 9. The highest 1,2-DCA concentration was only measured at 3 μM in the bottom layer. The decline in 1,2-DCA concentration continued to be observed during the testing period, though irregular fluctuation was found in some monitoring wells. Extensive studies have indicated that 1,2-DCA is resistant to be reductively dechlorinated by palladized NZVI or conventional ZVI. The observation of the 1,2-DCA degradation, though not as effective as the VC degradation, suggested that a biodegradation is involved onsite. Furthermore, as shown in Fig. 9(d) inset, an increase in chloroethane concentrations indicated that 1,2-DCA was reduced to chloroethane in the middle layer. This observation is consistent with the considerate increase in ethane shown in Fig. 10. Because 1,2-DCA was reductively dechlorinated to chloroethane, it implied that a cometabolic reaction occurred in the middle layer [39]. The enhanced biodegradation may be attributed to the modification of the redox condition in the aquifer. As shown in Fig. 7, ORP values decreased from +200 mV to −400 mV after the injection of NZVI. The strong reducing conditions are beneficial to the anaerobic bioremediation while the surfactant further stimulates microbial growth.

The evidence of NZVI-enhanced bioremediation is further revealed in Fig. 10. The concentrations of hydrocarbons and total organic carbon were measured along the downstream direction in the middle layer during Round 2. A high concentration of ethylene was determined in the testing site. The observation is consistent with the findings from Zemb et al. [40], suggesting that the appropriate bacteria such as *Dehalobacter* species are capable of reducing 1,2-DCA to ethylene when hydrogen gas was provided as electron donors under near neutral pH conditions.

The gradual increase in TOC concentrations followed by a subsequent leveling off suggested that the added biodegradable surfactant serves as the carbon source to stimulate microbial growth. Similar results have been documented in the literature where the surfactant also stimulated microbial growth when it

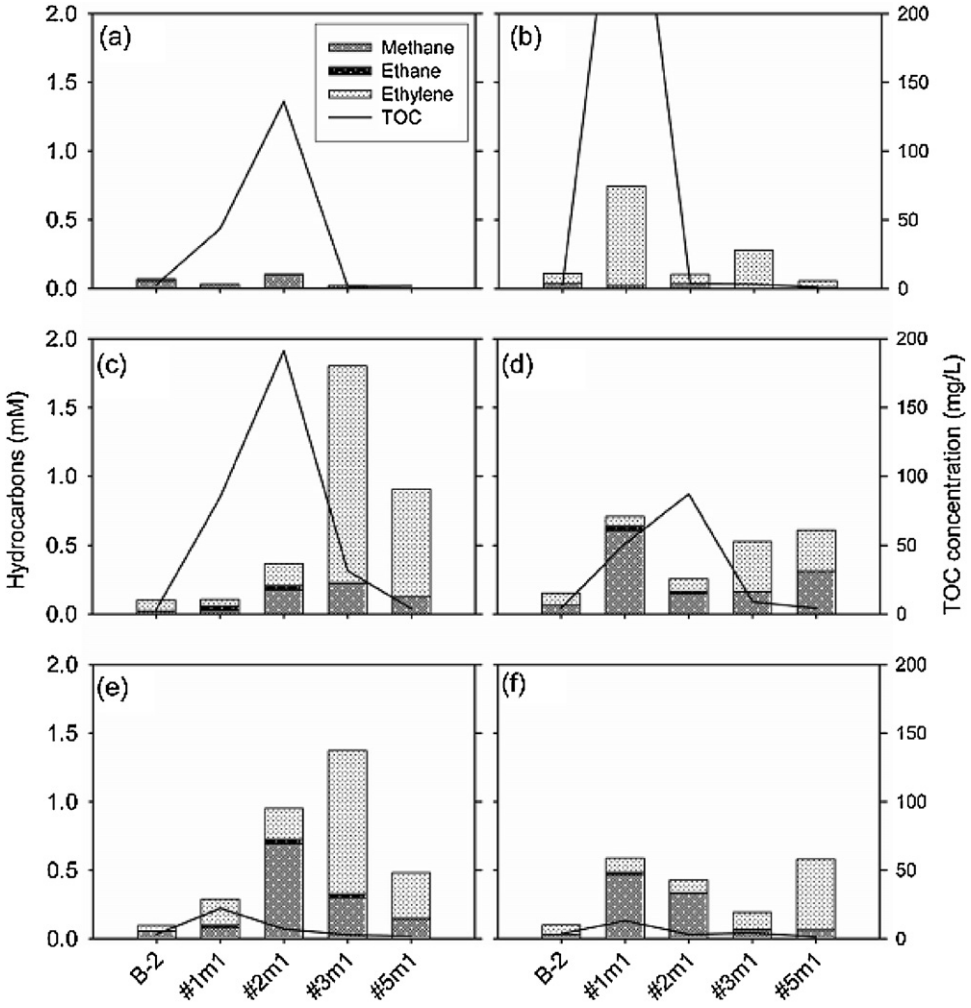

Fig. 10. Concentrations of TOC, methane, ethane and ethylene measured in the middle layers in Round 2 (a) Day 4 (b) Day 11 (c) Day 25 (d) Day 36 (e) Day 63 (f) Day 97.

was used to flush contaminants [41]. Compared to the less efficient degradation of 1,2-DCA by PAA-stabilized commercial NZVI in Round 1 where the polymer is less biodegradable (Fig. 9), 1,2-DCA concentrations maintained at a relatively low level in Round 2 is another evidence of enhanced bioremediation occurring after the injection of the biodegradable surfactant-stabilized NZVI. A synergistic effect coupling the biotic and abiotic processes may be involved in the in situ remediation of VC and 1,2-DCA using the biodegradable surfactant stabilized NZVI.

4. Conclusion

In this work, the surfactant stabilized NZVI was shown capable of remediating VC and 1,2-DCA through both biotic and abiotic processes. It is evident that both iron-mediated and biological processes exhibited significant effects on the degradation of contaminants using palladized NZVI stabilized with the biodegradable surfactant. From monitoring the iron concentration breakthrough and its distribution at the testing site, it was found that most NZVI had a tendency to stay in the upper layer with the gravity injection. In addition, ORP and pH results revealed that the test plot was in methanogenic conditions. The analysis of VC, 1,2-DCA and hydrocarbon concentrations indicated the transformation processes occurred in the test plot. The addition of the biodegradable surfactant not only promoted NZVI stability but also provided substrates to stimulate biological processes at this site.

Acknowledgements

The authors would like to thank the National Science Council (NSC), Taiwan, R.O.C. for the financial support under grant nos. NSC 95-2221-E-002-162-MY2 and NSC95-2221-E-390-014-MY2. We also like to thank Chinese Petroleum Corporation for its on-site assistance.

References

[1] X. Li, D.W. Elliott, W.-X. Zhang, Zero-valent iron nanoparticles for abatement of environmental pollutants: materials and engineering aspects, Crit. Rev. Solid State Mater. Sci. 31 (2006) 111–122.
[2] W.-X. Zhang, Nanoscale iron particles for environmental remediation: an overview, J. Nanopart. Res. 5 (2003) 323–332.
[3] H.-L. Lien, Y.-S. Jhuo, L.-H. Chen, Effect of heavy metals on dechlorination of carbon tetrachloride by iron nanoparticles, Environ. Eng. Sci. 24 (2007) 21–30.
[4] J. Feng, T. Lim, Pathways and kinetics of carbon tetrachloride and chloroform reductions by nano-scale Fe and Fe/Ni particles: comparison with commercial micro-scale Fe and Zn, Chemosphere 59 (2005) 1267–1277.
[5] H. Song, E.R. Carraway, Reduction of chlorinated ethanes by nanosized zero-valent iron: kinetics pathways, and effects of reaction conditions, Environ. Sci. Technol. 39 (2005) 6237–6245.
[6] Y. Liu, S.A. Majetich, R.D. Tilton, D.S. Sholl, G.V. Lowry, TCE dechlorination rates, pathways, and efficiency of nanoscale iron particles with different properties, Environ. Sci. Technol. 39 (2005) 1338–1345.
[7] H.-L. Lien, W.-X. Zhang, Nanoscale Pd/Fe bimetallic particles: catalytic effects of palladium on hydrodechlorination, Appl. Catal. B: Environ. 77 (2007) 110–116.
[8] D. Alessi, Z. Li, Synergistic effect of cationic surfactants on perchloroethylene degradation by zero-valent iron, Environ. Sci. Technol. 35 (2001) 3713–3717.

[9] L. Guo, Q. Huang, X.Y. Li, S. Yang, Iron nanoparticles: synthesis and applications in surface enhanced Raman scattering and electrocatalysis, Phys. Chem. 3 (2001) 1661–1665.
[10] P.F. Zhang, X. Tao, Z.H. Li, R.S. Bowman, Enhanced perchloroethylene reduction in column systems using surfactant-modified zeolite/zero-valent iron pellets, Environ. Sci. Technol. 36 (2002) 3597–3603.
[11] T. Phenrat, N. Saleh, K. Sirk, H.J. Kim, R.D. Tilton, G.V. Lowry, Stabilization of aqueous nanoscale zerovalent iron dispersions by anionic polyelectrolytes: adsorbed anionic polyelectrolyte layer properties and their effect on aggregation and sedimentation, J. Nanopart. Res. 10 (2008) 795–814.
[12] B. Schrick, B.W. Hydutsky, J.L. Blough, T.E. Mallouk, Delivery vehicles for zerovalent metal nanoparticles in soil and groundwater, Chem. Mater. 16 (2004) 2187–2193.
[13] P. Jiemvarangkul, W.-X. Zhang, H.-L. Lien, Enhanced transport of polyelectrolyte stabilized nanoscale zero-valent iron (nZVI) in porous media, Chem. Eng. J. 170 (2011) 482–491.
[14] N. Saleh, T. Phenrat, K. Sirk, B. Dufour, J. Ok, T. Sarbu, K. Matyjaszewski, R.D. Tilton, G.V. Lowry, Adsorbed triblock copolymers deliver reactive iron nanoparticles to the oil/water interface, Nano Lett. 5 (2005) 2489–2494.
[15] A. Tiraferri, K.L. Chen, R. Sethi, M. Elimelech, Reduced aggregation and sedimentation of zero-valent iron nanoparticles in the presence of guar gum, J. Colloid Interface Sci. 324 (2008) 71–79.
[16] F. He, D. Zhao, Preparation and characterization of a new class of starch-stabilized bimetallic nanoparticles for degradation of chlorinated hydrocarbons in water, Environ. Sci. Technol. 39 (2005) 3314–3320.
[17] M.J. Borda, R. Venkatakrishnan, F. Gheorghiu, Status of nZVI technology: lessons learned from North American and international field implementations, in: C.L. Geiger, K.M. Carvalho-Knighton (Eds.), Environmental Applications of Nanoscale and Microscale Reactive Metal Particles, ACS Symposium Series 1027, American Chemical Society, Washington, DC, 2009, pp. 219–232.
[18] D. Elliott, W.-X. Zhang, Field assessment of nanoscale bimetallic particles for groundwater treatment, Environ. Sci. Technol. 35 (2001) 4922–4926.
[19] Y.-T. Wei, S.-C. Wu, C.-M. Chou, C.-H. Che, S.-M. Tsai, H.-L. Lien, Influence of nanoscale zero-valent iron on geochemical properties of groundwater and vinyl chloride degradation: a field case study, Water Res. 44 (2010) 131–140.
[20] J.L. Berna, G. Cassani, C.-D. Hager, N. Rehman, I. Lopez, D. Schowanek, J. Steber, K. Taeger, T. Wind, Anaerobic biodegradation of surfactants – scientific review, Tenside Surf. Det. 44 (2007) 312–347.
[21] M. Elsner, M. Chartrand, N. Vanstone, G.L. Couloume, B.S. Lollar, Identifying abiotic chlorinated ethene degradation: characteristic isotope patterns in reaction products with nanoscale zero-valent iron, Environ. Sci. Technol. 42 (2008) 5963–5970.
[22] H. Song, E.R. Carraway, Catalytic hydrodechlorination of chlorinated ethenes by nanoscale zero-valent iron, Appl. Catal. B: Environ. 78 (2008) 53–60.
[23] H.-L. Lien, W.-X. Zhang, Hydrodechlorination of chlorinated ethanes by nanoscale Pd/Fe bimetallic particles, J. Environ. Eng. 131 (2005) 4–10.
[24] R. Lookman, L. Bastiaens, B. Borremans, M. Maesen, J. Gemoets, L. Diels, Batch-test study on the dechlorination of 1,1,1-trichloroethane in contaminated aquifer material by zero-valent iron, J. Contam. Hydrol. 74 (2004) 133–144.
[25] U.S. EPA., Technical guidance for the natural attenuation indicators: methane, ethane, and ethene, New England, 2002.
[26] Y.-T. Wei, S.-C. Wu, Development of a trajectory model for predicting attachment of submicrometer particles in porous media: stabilized NZVI as a case study, Environ. Sci. Technol. 44 (2010) 8996–9002.
[27] T. Madsen, H. Buchardt, D. Boyd, A. Nylén, R. Pedersen, G.I. Petersen, F. Simonsen, Environmental and health assessment of substances in household detergents and cosmetic detergent products, Environmental Project No. 615, Danish Environmental Protection Agency, 2001.
[28] J.R. Larsen, T.T. Andersen, Survey of liquid hand soaps, including health and environmental assessments, Survey of Chemical Substances in Consumer Products No. 69, Danish Environmental Protection Agency, 2006.
[29] K. Hanaki, T. Mastsuo, M. Nagase, Mechanism of inhibition caused by long chain fatty acids in anaerobic digestion process, Biotechnol. Bioeng. 23 (1981) 1591–1610.
[30] I.W. Koster, A. Cramer, Inhibition of methanogenesis from acetate in granular sludge by long-chain fatty acids, Appl. Environ. Microbiol. 53 (1987) 403–409.
[31] K.M. Yao, M.T. Habibian, C.R. O'Melia, Water and wastewater filtration: concepts and applications, Environ. Sci. Technol. 5 (1971) 1105–1112.
[32] G.A. Loraine, Effects of alcohols, anionic and nonionic surfactants on the reduction of TCE by zero-valent iron, Water Res. 35 (2001) 1453–1460.
[33] P. Bradley, F. Chapelle, D. Lovley, Humic acids as electron acceptors for anaerobic microbial oxidation of vinyl chloride and dichloroethene, Appl. Environ. Microbiol. 64 (1998) 3102–3105.
[34] M.R. Kriegman-King, M. Reinhard, Transformation of carbon tetrachloride in the presence of sulfide, biotite, and vermiculite, Environ. Sci. Technol. 26 (1992) 2198–2206.
[35] R.W. Gllham, S.F. O'Hannesin, Enhanced degradation of halogenated aliphatics by zero-valent iron, Ground Water 32 (1994) 958–967.
[36] R. Nobre, M. Nobre, Natural attenuation of chlorinated organics in a shallow sand aquifer, J. Hazard. Mater. 110 (2004) 129–137.
[37] T.H. Wiedemeier, J.T. Wilson, D. Kampbell, J.E. Jansen, P. Haas, Technical protocol for evaluating the natural attenuation of chlorinated ethenes in groundwater, in: Proceedings of the 1996 Petroleum Hydrocarbons and Organic Chemicals in Ground Water: Prevention, Detection, and Remediation Conference, Natural Water and Well Association, Houston TX, USA, 1996, pp. 425–444.
[38] X. Maymo-Gatell, T. Anguish, S.H. Zinder, Reductive dechlorination of chlorinated ethenes and 1,2-dichloroethane by dehalococcoides ethanogenes 195, Appl. Environ. Microbiol. 65 (1999) 3108–3113.
[39] C. Holliger, G. Schraa, E. Stupperich, A.J. Stams, A.J. Zehnder, Evidence for the involvement of corrinoids and factor F430 in the reductive dechlorination of 1,2-dichloroethane by Metbanosarcina barked, J. Bacteriol. 174 (1992) 4427–4434.
[40] O. Zemb, M. Lee, A. Low, M. Manefield, Reactive iron barriers: a niche enabling microbial dehalorespiration of 1,2-dichloroethane, Appl. Microbiol. Biotechnol. 88 (2010) 319–325.
[41] C.A. Ramsburg, L.M. Abriola, K.D. Pennell, F.E. Loffler, M. Gamache, B.K. Amos, E.A. Petrovskis, Stimulated microbial reductive dechlorination following surfactant treatment at the Bachman Road site, Environ. Sci. Technol. 38 (2004) 5902–5914.